

Absorption and photoemission spectroscopy of rare-earth oxypnictides

To cite this article: T Kroll *et al* 2009 *New J. Phys.* **11** 025019

View the [article online](#) for updates and enhancements.

Related content

- [Te concentration dependent photoemission and inverse-photoemission study of FeSe_{1-x}Te_x](#)
Takayoshi Yokoya, Rikiya Yoshida, Yuki Utsumi *et al.*
- [Strong hybridization in vanadium oxides: evidence from photoemission and absorption spectroscopy](#)
R Zimmermann, R Claessen, F Reinert *et al.*
- [Effect of 3d doping on the electronic structure of BaFe₂As₂](#)
J A McLeod, A Buling, R J Green *et al.*

Recent citations

- [Anderson's impurity-model analysis on CeO_{1-x}F_xBiS₂](#)
Takuya Sugimoto *et al*
- [The iron L edges: Fe 2p X-ray absorption and electron energy loss spectroscopy](#)
Piter S. Miedema and Frank M.F. de Groot
- [Observation of two-hole satellite in the resonant x-ray photoemission spectra of Ba_{1-x}K_xFe₂As₂ single crystals](#)
A. Koitzsch *et al*

Absorption and photoemission spectroscopy of rare-earth oxypnictides

T Kroll^{1,3}, F Roth¹, A Koitzsch¹, R Kraus¹, D R Batchelor²,
J Werner¹, G Behr¹, B Büchner¹ and M Knupfer¹

¹ IFW Dresden, PO Box 270016, D-01171 Dresden, Germany

² Forschungszentrum Karlsruhe, Institut für Synchrotronstrahlung,
D-76021 Karlsruhe, Germany

E-mail: t.kroll@ifw-dresden.de

New Journal of Physics **11** (2009) 025019 (11pp)

Received 24 October 2008

Published 27 February 2009

Online at <http://www.njp.org/>

doi:10.1088/1367-2630/11/2/025019

Abstract. The electronic structure of various rare-earth oxypnictides has been investigated by performing Fe $L_{2,3}$ x-ray absorption spectroscopy, and Fe 2p and valence band x-ray photoemission spectroscopy. As representative samples the non-superconducting parent compounds $LnFeAsO$ ($Ln = La, Ce, Sm$ and Gd) have been chosen and measured at 25 and 300 K, i.e. below and above the structural and magnetic phase transition at ~ 150 K. We find no significant change of the electronic structure of the FeAs layers when switching between the different rare-earth ions or when varying the temperature below and above the transition temperatures. Using a simple two-configuration model, we find qualitative agreement with the Fe $2p_{3/2}$ core-level spectrum, which allows for a qualitative explanation of the experimental spectral shapes.

³ Author to whom any correspondence should be addressed.

Contents

1. Introduction	2
2. Experiment	3
3. Results	4
3.1. Rare-earth absorption spectra	4
3.2. Fe $L_{2,3}$ -absorption edges	4
3.3. Fe 2p and valence band photoemission	5
4. Discussion	7
5. Summary	9
Acknowledgments	10
References	10

1. Introduction

The discovery of high-temperature superconductivity in $\text{LaFeAsO}_{1-x}\text{F}_x$ at the beginning of 2008 [1] has generated much excitement and stimulated enormous scientific efforts. Superconductivity emerges when electrons are doped into the FeAs layers either by chemical substitution of fluorine for oxygen [1], or by oxygen deficiencies [2, 3]. Also hole doping into the FeAs layers has been reported with superconductivity at 25 K [4]. In fact, a large oxypnictide family $L_n\text{FeAsO}$ ($L_n = \text{La, Ce, Pr, Nd, Sm}$ and Gd) has been found to be superconducting with a transition temperature up to 55 K [3]–[6] and high upper critical fields [7, 8]. The onset of the superconducting critical temperature (T_c) in these compounds increases with the reduction of the rare-earth ionic size, and the highest T_c obtained so far is 55 K in SmFeAsO [3, 5]. Interestingly enough, this maximum value could not be increased by applying external pressure. F-doped $\text{LaFeAsO}_{1-x}\text{F}_x$ shows an increasing transition temperature T_c from 28 to 43 K at 4 GPa, but T_c decreases monotonically above 4 GPa and is lowered below 10 K at 31 GPa [9]. In contrast, superconducting $\text{NdFeAsO}_{0.6}$ (nominal composition) with a T_c of 54 K at ambient pressure shows a monotonic decrease of T_c up to the highest experimental external pressure of 18 GPa [10].

In the low doping regime, a magnetic and structural phase transition takes place at around 150 K for all rare-earth ions in $L_n\text{FeAsO}$. The magnetic structure of the oxypnictides within the a – b -plane consists of chains of parallel Fe spins that are coupled antiferromagnetically in the orthogonal direction, with an ordered moment substantially less than $1 \mu_B$ per iron [11]–[15].

The knowledge of the electronic structure is a precondition for any advanced understanding of all physical properties. In particular, it is of high interest to know the fundamental correlation parameters that determine the electronic structure. In LaCoO_3 , for example, an energetic proximity between the low-spin ground state and an intermediate- or high-spin state has been found [16]–[18], which results in a clearly visible temperature-dependent x-ray absorption spectroscopy (XAS) signal [17]. In principle, a structural phase transition may lead to different ligand field parameters that become visible in XAS and x-ray photoemission spectroscopy (XPS) measurements. The exchange of rare-earth ions also has an effect on the crystal structure and therefore may also have an effect on the electronic structure. However, if a phase transition does not change the orbital occupation (e.g. the spin state), but only affects the spatial arrangements, changes may become invisible since $t_{pd} \sim r^{-7/2}$.

Core level spectroscopic measurements such as XAS and XPS are appropriate experimental methods to enhance our knowledge about the dependence of the electronic structure on the Ln ion. These methods are complementary to each other and reveal valuable information about the electronic structure. Several publications have already presented results on the electronic structure of $LaFeAsO_{1-x}F_x$ using core level spectroscopy: a soft x-ray absorption study of the O K and Fe $L_{2,3}$ edge finds a doping-dependent shift of the chemical potential visible on both edges. From a comparison of the O K edge spectra to local density approximation (LDA)-based bandstructure, it is concluded that the electronic structure is bandwidth dominated. Furthermore, simulations of the Fe $L_{2,3}$ edge spectra by charge transfer multiplet calculations reveal a multiplet-averaged value of $U_{dd} = 1.5$ eV [19]. Different articles report on photoemission data. Koitzsch *et al* present results from the photon energy dependence of the valence band spectra and conclude that the low-energy peak is derived almost exclusively from Fe 3d states. With electron doping they find a shift of the La 4d core levels towards higher energies, which they attribute to a shift of the chemical potential with electron doping [20]. A recent XPS paper investigates the Fe 2p core levels and the Fe 3p–3d resonant photoemission process [21]. The data are consistent with a less correlated picture as well. Kurmaev *et al* [22] report on x-ray emission and XAS experiments, and also support a picture without strong correlations.

In this paper, we present XAS and XPS data on $LnFeAsO$ ($Ln = La, Ce, Sm$ and Gd) polycrystalline samples at temperatures above (300 K) and below (25 K) the phase transition temperatures ($T \approx 150$ K) and compare them with a two-configuration model.

2. Experiment

Polycrystalline samples of $LnFeAsO$ ($Ln = La, Ce, Sm$ and Gd) were prepared from pure components (3N or better) by using a two-step solid-state reaction method, similar to that described by Zhu *et al* [23]. In the first step, Fe powder and powdered As particles were milled, mixed and pressed into pellets under Ar atmosphere, and annealed at 500 °C for 2 h and at 700 °C for 10 h in an evacuated silica tube. In the second step, the FeAs pellets were milled and mixed with Ln powder, annealed Ln_2O_3 powder and subsequently pressed into pellets under a well-defined pressure. Then, the samples were heated in an evacuated silica tube at 940 °C for 2 h and at 1150 °C for 48 h. To improve the homogeneity, the 940 °C annealing step was prolonged to 8 h. The annealed pellets were ground and polished, and the local composition of the resulting samples was investigated by wavelength-dispersive x-ray spectroscopy (WDX) in a scanning electron microscope. The samples consist of 1–100 μm sized grains of $LnFeAsO$. They have been characterized by x-ray diffraction, magnetization, transport and local probes such as muon spin relaxation (μSR) and nuclear magnetic resonance (NMR) measurements [24].

XAS and XPS studies at the O K -, $Ln M_{4,5}$ - and Fe $L_{2,3}$ -edges as well as at the Fe 2p and valence band excitations were performed at the UE52-PGM beamline of the synchrotron radiation source Bessy II. The energy resolution was set to 60, 90, 115, 125 and 155 meV at 530 (O K), 710 (Fe L), 840 (La M), 890 (Ce M) and 1020 eV photon energy (Sm M), respectively. Data were recorded by measuring the partial electron yield (PEY) signal that has been taken by using a multi-channel plate detector. In order to obtain appropriate surfaces, the pellets were filed *in situ* in a vacuum environment of 10^{-8} mbar and measured at 10^{-10} mbar.

The photon and binding energies (XAS and XPS, respectively) are referenced to the Au 4f binding energy throughout the paper unless indicated otherwise.

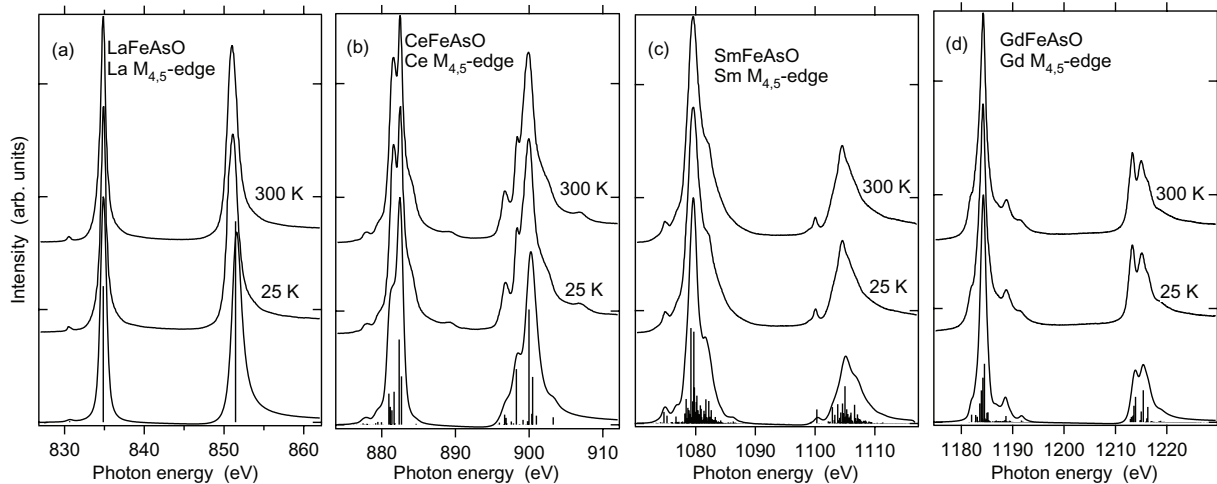


Figure 1. Comparison of experimental XAS spectra of the $Ln M_{4,5}$ edge at 25 and 300 K and corresponding multiplet calculations (bottom spectra): (a) LaFeAsO, (b) CeFeAsO, (c) SmFeAsO and (d) GdFeAsO. No spectral variations are visible as a function of temperature, the theoretical spectra match the experimental spectra very well which emphasizes the validity of the simple picture commonly used for the rare-earth series also in this compound.

3. Results

3.1. Rare-earth absorption spectra

A common way to assign the formal valences is $Ln^{3+}Fe^{2+}As^{3-}O^{2-}$, which leaves Fe as $3d^6$, As as $4p^6$ and O as $2p^6$ ions. These formal valences may change due to hybridization processes, especially at Fe and As [19]. The number of electrons in the 4f shell of the rare-earth ions depends on their atomic number. Formally, it is La: $4f^0$, Ce: $4f^1$, Sm: $4f^5$ and Gd: $4f^7$. Since the 4f shell is screened by the fully occupied 5s and 5p shells, it can be treated as not interacting with its environment, i.e. the influence of the crystal field can be neglected. In figure 1, the experimental $M_{4,5}$ absorption edges at 25 and 300 K are compared with theoretical calculations. Here, $M_{4,5}$ refers to excitations from a 3d core level ($J = 3/2$: M_4 and $J = 5/2$: M_5) into unoccupied 4f states. When neglecting crystal field effects, a description using spherical symmetry should be sufficient in order to explain the experimental spectra. To do so, we performed atomic multiplet calculations for La, Ce, Sm and Gd $M_{4,5}$ absorption edges using spherical symmetry [25, 26]. For better comparability, the theoretical intensities have been broadened by a Gaussian of 0.25 eV half-width at half-maximum (HWHM) and a Lorentzian of 0.25 eV (M_5) and 0.6 eV (M_4) (HWHM) due to different lifetime broadenings. As can be observed in figure 1, these simple calculations match the experimental spectra very well, which emphasizes the validity of the common picture of the rare-earth ion and its valence as 3+ for all rare-earth ions tested and at different temperatures.

3.2. Fe $L_{2,3}$ -absorption edges

According to the dipole selection rules the Fe $L_{2,3}$ excitations as probed by these experiments, correspond to core electron transitions into unoccupied Fe 3d electronic states, i.e. the density

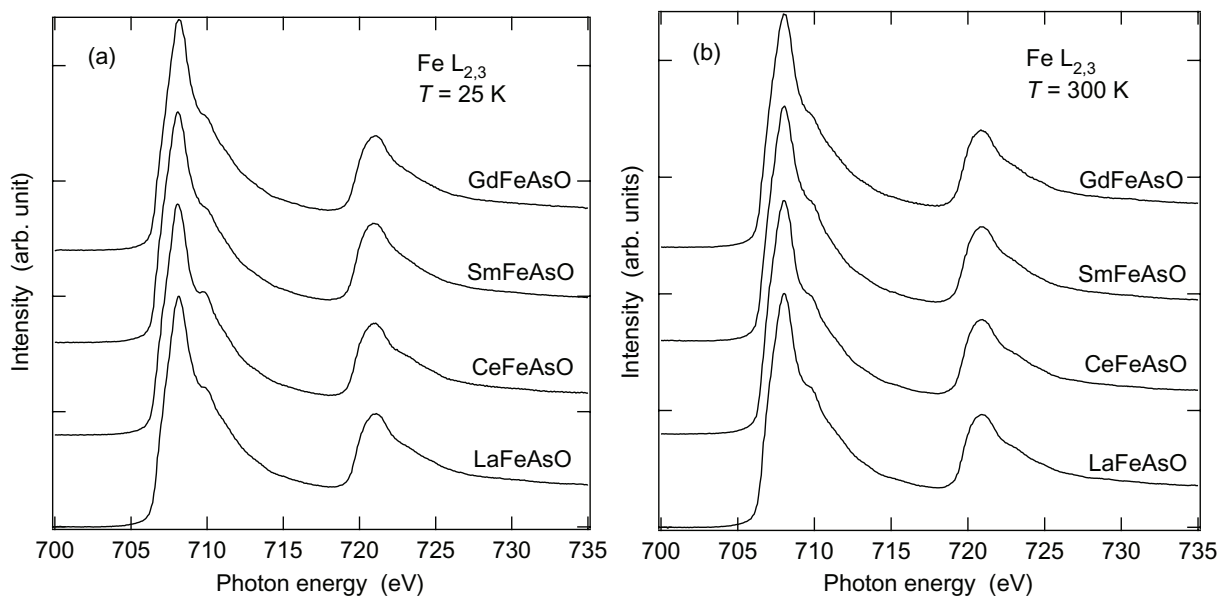


Figure 2. Fe $L_{2,3}$ absorption edges for the four different $LnFeAsO$ systems at 25 (a) and 300 K (b). No significant changes of the spectral shape are visible for any of the curves.

of states (DOS) of the unoccupied states is probed. We performed measurements of the Fe $L_{2,3}$ absorption edge on undoped $LnFeAsO$ ($Ln=La, Ce, Sm$ and Gd) polycrystalline samples at two different temperatures: 25 and 300 K. The two chosen temperatures are well below and above these transition temperatures at ≈ 150 K and changes of the electronic structure should become visible. In figures 2(a) and (b), the Fe $L_{2,3}$ edge spectra at 25 and 300 K, respectively, are shown for the four different samples. As can be seen, no obvious changes are visible. All eight spectra consist of a main peak around 708.1 eV and a shoulder ≈ 1.5 eV higher in energy at the L_3 edge, similar at the L_2 edge. Since the exchange of the rare-earth ions does not change the formal valence, and all systems have the same generic phase diagram, no strong changes are expected. Since the formal Fe valence remains unchanged, the only possible changes can occur due to different Fe–As hopping and different local distortions of the tetrahedron surrounding one Fe ion, but none of these possible influences become visible in the x-ray absorption spectra.

3.3. Fe 2p and valence band photoemission

In a photoemission process, a core or valence electron is excited into the vacuum. Therefore, one probes the occupied states of a system complementary to the absorption process. But similar to XAS, one is sensitive to changes in the electronic structure, especially to differences in the hopping parameters between the central Fe ion and its surrounding As ligands. Figures 3(a) and (b) present a compilation of Fe 2p spectra of the series $LnOFeAs$ ($Ln = La, Ce, Sm$ and Gd) at 25 and 300 K, respectively. The spectra consist of the Fe $2p_{3/2}$ peak at $E = 706.6$ eV and the Fe $2p_{1/2}$ peak at $E = 719.8$ eV. The principal structure of the spectra does not change. We find a narrow but asymmetric Fe $2p_{3/2}$ peak and no strong separate satellite but a weak shoulder at $E \approx 710$ eV. However, at room temperature, the weak shoulder seems to weaken even more when going from La to Gd, where it is almost invisible. Interestingly enough, such

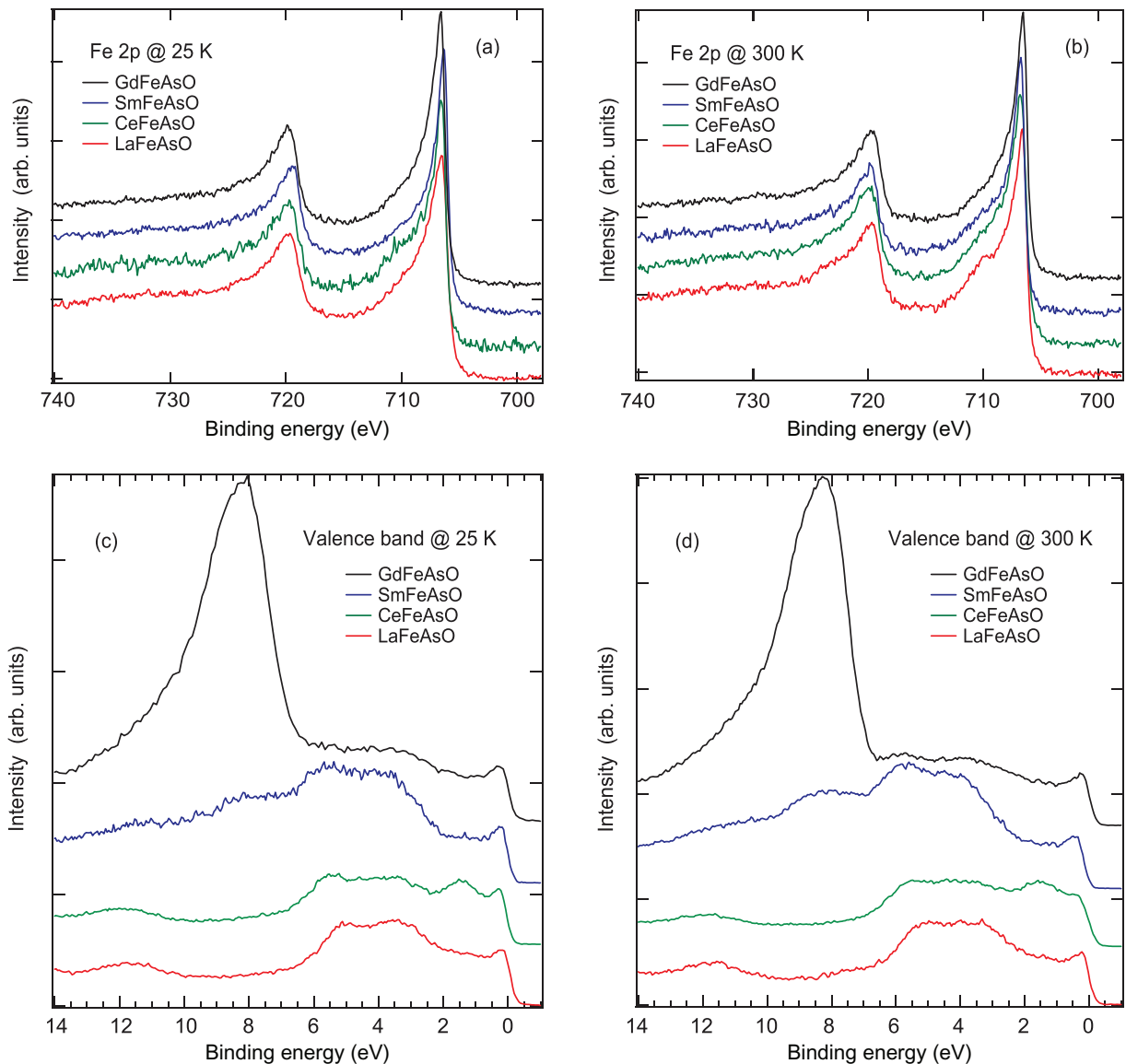


Figure 3. Comparison of experimental core level and valence band photoemission spectroscopy data. (a) and (b) The Fe 2p excitation spectra at 25 and 300 K, respectively. Equivalently, (c) and (d) show the valence band photoemission data.

behaviour has not been observed at 25 K. By substituting La by lanthanides of increasing atomic weight, the lattice shrinks due to the well-known lanthanide contraction. Smaller bond lengths favour larger hopping parameters, which would imply an increased satellite–main line distance, contradictory to the experimental observations. However, the most likely explanation is that the multiplets are somewhat different across the series causing different line shapes.

In figures 3(c) and (d), the valence band photoemission spectra of $L_n\text{FeAsO}$ are shown for 25 and 300 K, respectively. In [20], the valence band spectra of LaFeAsO have been nicely explained by the DOS as calculated in the LDA [27]. It turned out that the low-energy states are

dominated by Fe 3d states with almost no admixture of As 4p states. The broad peak around 4 eV consists of at least two features. The lower one around 3.5 eV contains spectral weight of various atomic species (including Fe), whereas the high-energy feature around 5 eV is dominated by excitations from oxygen.

A comparison of LaFeAsO to the other rare-earth oxypnictides is only qualitatively possible, due to the existence of additional rare-earth emission lines. Due to these additional peaks, a reasonable normalization of the spectra is difficult. Therefore, all data have been normalized at the low-energy peak at ~ 0.21 eV where only Fe states are present. Beginning with CeFeAsO, its valence band emission spectrum shows the same features as LaFeAsO, beside a small peak at ~ 1.2 eV. This peak can be assigned to Ce 4f¹ emission as it has been found also in other compounds earlier [28]. The Sm 4f⁵ emission is known to appear between 5 and 10 eV binding energy [29] and can be assigned to the broad peak around 8 eV in the SmFeAsO spectrum. The GdFeAsO valence band spectrum is dominated by an intensive peak at 8.2 eV and is well known to originate from the Gd 5p excitation. Beside these additional features caused by rare-earth excitations, the overall spectral shape remains unchanged for all L_n FeAsO spectra. This observation is in agreement with the Fe $L_{2,3}$ edge absorption and 2p photoemission results and emphasizes that an exchange of rare-earth ions in the oxypnictide family does not change the electronic structure in the FeAs layers. Since the above argumentation holds true for both temperatures tested, one can conclude that the magnetic and structural phase transition does not affect the electronic structure of the FeAs layers as seen by these experiments.

4. Discussion

As mentioned above, the unoccupied DOS is probed in an XAS experiment. Therefore, the spectral shape is mostly sensitive to the interactions in the final state, i.e. after exciting a Fe 2p core electron of a certain ground state into an unoccupied Fe 3d state leaving a Fe 2p core hole behind. In [19], such a scenario has been simulated for fluorescence yield data of LaFeAsO by applying charge transfer multiplet calculations in tetrahedral symmetry T_d . Summarized, they find weak correlations ($U = 1.5$ eV, multiplet averaged), small hopping ($|\text{pd}\pi| = 0.27$ eV) and crystal field parameters ($10Dq = 0.2$ eV), and a small charge transfer energy gap $\Delta = 1.25$ eV, where Δ is defined as the energy difference between the lowest lying states of the $3d^7\bar{L}$ and the $3d^6$ multiplets, \bar{L} denotes a ligand hole. According to the spectra shown in figure 2, these values do not change significantly when replacing La by Ce, Sm or Gd, or when varying the temperature above and below the transition temperatures T_S and T_N . The same observation holds true for the Fe 2p and valence band photoemission spectra, where no significant changes can be observed.

As long as the transition does not affect the orbital occupancy, simple changes of the hopping parameter are invisible within the used resolution, since $t_{\text{pd}} \sim r^{-7/2}$. In fact, recent publications using angle-resolved photoemission spectroscopy (ARPES) suggest an exchange splitting of the band structure as the origin of the magnetic phase transition [30, 31], which would clearly be invisible in angle-integrated XPS as used during this investigation.

When discussing the Fe 2p photoemission spectra (figures 3(a) and (b)), the most important feature of these spectra is the absence of an obvious satellite structure typically observed for many transition metal compounds [32]. Closer inspection, however, reveals an asymmetric line shape, especially of the Fe 2p_{3/2} peak, which leaves room for the possibility that the satellite is situated close to the main line and both peaks almost merge. The satellite intensity is a measure

of the degree of change in the hybridization state of the system when the initial state is compared with the photoemission final state. In the simplest case, where only two energy levels are considered, the ground state can be described by the wavefunction $\psi = (\cos \theta)d^6 - (\sin \theta)d^7\bar{L}$, where \bar{L} refers to a hole at the ligand orbitals As 4p. The photoemission final state corresponds to $\psi_S = (\sin \theta')cd^6 + (\cos \theta')cd^7\bar{L}$ and $\psi_M = (\cos \theta')cd^6 - (\sin \theta')cd^7\bar{L}$, where c refers to a hole in the core level (here the 2p shell) created by the photoemission process, S and M refer to the satellite and main line, respectively. Within the well-known two-configuration model introduced by van der Laan *et al* [32] the satellite to main line intensity ratio is

$$\frac{I_S}{I_M} = \tan^2(\theta' - \theta) \quad (1)$$

and the energy splitting is

$$\Delta E = \sqrt{(\Delta - U_{dc})^2 + 4V_{\text{eff}}^2}, \quad (2)$$

where Δ is the charge transfer energy, U_{dc} is the on-site energy between the core hole and the d-shell and V_{eff} is the effective hybridization parameter between d^6 and $d^7\bar{L}$ states. The relative weighing of the d^6 and $d^7\bar{L}$ configurations in the final state will strongly change relative to the ground state if the Coulomb energy U_{dc} is large since this favours the $d^7\bar{L}$ configuration because here the additional d-electron efficiently screens the core hole. According to formula (1) this tends to increase the satellite intensity. The spectra in figure 3(a) and (b) suggest, on the other hand, that the satellite intensity is rather low and the energy separation from the main line is small. From this a rather small value of the on-site energy U_{dc} can be inferred which also points to a low value of the on-site Hubbard repulsion U_{dd} since both quantities are affected similarly by screening effects. In figure 4, we follow the above reasoning in a more quantitative manner. Using $U_{dd} = 1.5$ eV (multiplet averaged), $U_{dc} = U_{dd} + 1$ eV, $\Delta = 0.0$ eV and $V_{\text{eff}} = \sqrt{V_e^2 + 3V_{t_2}^2} = 1.39$ eV (for $S = 2$ in T_d symmetry), we obtain $I_S/I_M = 0.15$ and $\Delta E = 3.7$ eV. Note that $\Delta = 0.0$ refers to the energy difference of the centres of gravity of d^6 and $d^7\bar{L}$ configurations, while in [19], $\Delta = 1.25$ eV refers to the difference between the lowest lying states of d^6 and $d^7\bar{L}$ of the full multiplet splitting. The relative weight and the energy separation of satellite and main line are shown in figure 4 by bars. We find qualitative agreement with experiment. The exact line shape can, of course, not be described correctly by this coarse modelling since e.g. any multiplet effects are neglected.

In the local picture, the small splitting values $10Dq$, $|pd\pi|$ and $|pd\sigma|$ force the Fe states into a high-spin situation obeying Hund's first rule. Due to hybridization effects, the most important contributions to the ground state are $3d_{(e^3)(t_2^3)}^6$ and $3d_{(e^3)(t_2^4)}^6\bar{L}$. Note that in T_d symmetry it is $V_e = \frac{1}{\sqrt{3}}V_{t_2}$. Therefore, the ligand hole has mainly t_2 symmetry in contrast to what is used from, e.g., the cobaltites [33]. The energy difference between the two possible eigenstates in the two-configuration model for the one electron removal process (d^5 and $d^6\bar{L}$) is $\Delta E = \sqrt{(\Delta - U_{dd})^2 + 4V_{\text{eff}}^2}$, where $\Delta = E(d^7\bar{L}) - E(d^6)$. When looking at the first electron removal states as is present after a valence band photoemission process, there are two possibilities for the removed 3d electron: it may have either e or t_2 symmetry. In the first case, a configuration like $3d_{(e^2)(t_2^3)}^5$ has three empty t_2 and two empty e orbitals to hybridize with (i.e. $V_{\text{eff}} = 1.46$ eV), whereas in the latter case a configuration such as $3d_{(e^3)(t_2^2)}^5$ has four empty t_2 orbitals and one empty e orbital to hybridize with (i.e. $V_{\text{eff}} = 1.59$ eV). So these states would split by 3.3 and 3.5 eV, respectively. When comparing these results with the experimental valence band and

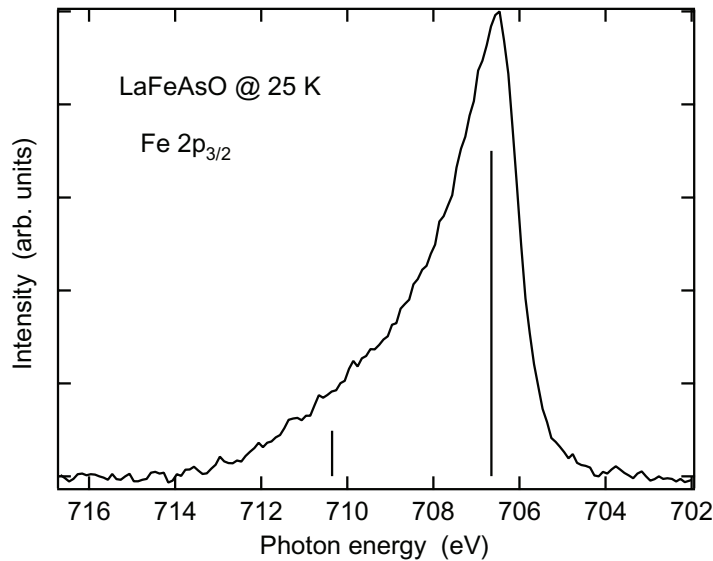


Figure 4. LaFeAsO Fe $2p_{3/2}$ photoemission spectrum at 25 K; for a better comparison to the theoretical model, a Shirley background has been subtracted. The vertical bars represent the energy position and relative intensity of the two states of the two configuration model (see text for further description).

DOS one finds additional Fe states between 2.0 and 3.6 eV below the low-energy peak in the photoemission (this work and [20]) and between 2.2 and 3.2 eV below the Fermi energy in the DOS results [20, 27]. Interestingly enough, these values match those derived from the local ansatz described above rather nicely. This is a somewhat surprising result, since it is well known that the oxypnictide family has pronounced itinerant character. Since in the valence band electron removal process no core hole comes into play, it seems questionable if a description using a local ansatz for the valence band photoemission spectra is correct. However, resonant photoemission data show that the feature at ≈ -3.6 eV is enhanced when driving the energy across the Fe L edge [34] confirming the applicability of the model.

5. Summary

In summary, we performed XAS at the Fe $L_{2,3}$ edge as well as core level Fe 2p and valence band photoemission spectroscopy for various rare-earth oxypnictides $Ln\text{FeAsO}$ ($Ln = \text{La, Ce, Sm and Gd}$) at temperatures above and below the phase transition temperatures. In none of our results do we find significant change of the spectral shape that leads to the conclusion that the electronic structure of the FeAs layers as seen by these experiments does not change by exchanging the rare-earth ions or varying the temperature.

For further interpretation, we compared the experimental results with a simple two-configuration model. Within this model, we are able to explain the absence of a strong satellite in the Fe 2p excitation spectrum as a consequence of a small on-site Coulomb energy U_{dc} between the 2p core hole and the 3d-shell. When applying the same model to the valence band spectrum, we find additional Fe 3d satellite excitations at 3.3 and 3.5 eV below the main (low-energy) peak. Interestingly, the experimental valence band as well as DOS show additional Fe states at

similar energies. These findings are somewhat surprising, since the validity of a local model as used here is not obvious. LnFeAsO has been identified as a metal, which would support an itinerant picture at least for the valence band description. Due to the existence of a Fe 2p core hole in the other experiments, a local description may be sufficient as long as U_{dc} is larger than the conduction bandwidth. From LDA calculations, a conduction bandwidth of ≈ 4 eV [27] has been found with a width of the unoccupied states of ≈ 2 eV. In this paper we use $U_{\text{dc}} = 2.5$ eV, which may be located at the border of validity. Note that any consequence of the influence of a possible polarizability of the As ions (beside a small U_{dd}) [35], is not included in any of the theoretical methods used in this paper. In the context of these arguments, it is a surprising but interesting point that the simple model as used in this work is still able to describe the experimental spectra.

Acknowledgments

We are grateful to R Hübel, S Leger and R Schönfelder for technical assistance. This investigation was supported by the DFG project SFB 463. TK has been financed by the DFG project KR 3611/1-1.

References

- [1] Kamihara Y, Watanabe T, Hirano M and Hosono H 2008 *J. Am. Chem. Soc.* **130** 3296
- [2] Yang J *et al* 2008 *Supercond. Sci. Technol.* **21** 082001
- [3] Kito H, Eisaki H and Iyo A 2008 *J. Phys. Soc. Japan* **77** 063707
- [4] Wen H-H, Mu G, Fang L, Yang H and Zhu X 2008 *Europhys. Lett.* **82** 17009
- [5] Ren Z-A, Yang J, Lu W, Yi W, Che G-C, Dong X-L, Sun L-L and Zhao Z-X 2008 *Mater. Res. Innov.* **12** 1
- [6] Chen X H, Wu T, Wu G, Liu R H, Chen H and Fang D F 2008 *Nature* **453** 761
- [7] Hunte F, Jaroszynski J, Gurevich A, Larbalestier D C, Jin R, Sefat A S, McGuire M A, Sales B C, Christen D K and Mandrus D 2008 *Nature* **453** 903
- [8] Fuchs G *et al* 2008 *Phys. Rev. Lett.* **101** 237003
- [9] Takahashi H, Igawa K, Arii K, Kamihara Y, Hirano M and Hosono H 2008 *Nature* **453** 376
- [10] Takeshita N, Iyo A, Eisaki H, Kito H and Ito T 2008 *J. Phys. Soc. Japan* **77** 075003
- [11] de la Cruz C *et al* 2008 *Nature* **453** 899
- [12] McGuire M A *et al* 2008 *Phys. Rev. B* **78** 094517
- [13] Chi S *et al* 2008 *Phys. Rev. Lett.* **101** 217002
- [14] Liu R H *et al* 2008 *Phys. Rev. Lett.* **101** 087001
- [15] Chen Y, Lynn J W, Li J, Li G, Chen G F, Luo J L, Wang N L, Dai P, de la Cruz C and Mook H A 2008 *Phys. Rev. B* **78** 064515
- [16] Korotin M A, Ezhov S Yu, Solovyev I V, Anisimov V I, Khomskii D I and Sawatzky G A 1996 *Phys. Rev. B* **54** 5309
- [17] Haverkort M W *et al* 2006 *Phys. Rev. Lett.* **97** 176405
- [18] Vanko G, Rueff J-P, Mattila A, Nemeth Z and Shukla A 2006 *Phys. Rev. B* **73** 024424
- [19] Kroll T *et al* 2008 *Phys. Rev. B* **78** 220502
- [20] Koitzsch A *et al* 2008 *Phys. Rev. B* **78** 180506
- [21] Malaeb W *et al* 2008 *J. Phys. Soc. Japan* **77** 093714
- [22] Kurmaev E Z, Wilks R G, Moewes A, Skorikov N A, Izyumov Yu A, Finkelstein L D, Li R H and Chen X H 2008 *Phys. Rev. B* **78** 220503
- [23] Zhu X, Yang H, Fang L, Mu G and Wen H-H 2008 *Supercond. Sci. Technol.* **21** 105001

- [24] Grafe H-J *et al* 2008 *Phys. Rev. Lett.* **101** 047003
- Klauss H H *et al* 2008 *Phys. Rev. Lett.* **101** 077005
- Luetkens H *et al* 2008 *Phys. Rev. Lett.* **101** 097009
- Klingeler R *et al* 2008 arXiv:0808.0708v1
- [25] Cowan R D 1981 *The Theory of Atomic Structure and Spectra* (Berkeley, CA: University of California Press)
- [26] de Groot F M F 2005 *Coord. Chem. Rev.* **249** 31
- [27] Eschrig H 2008 arXiv:0804.0186v2
- [28] Peterman D J, Weaver J H, Croft M and Peterson D T 1983 *Phys. Rev. B* **27** 808
- [29] Allen J W, Johansson L I, Bauer R S, Lindau I and Hagström S B M 1978 *Phys. Rev. Lett.* **41** 1499
- [30] Yang L X *et al* 2008 arXiv:0806.2627
- [31] Zhang Y *et al* 2008 arXiv:0808.2738
- [32] van der Laan G, Westra C, Haas C and Sawatzky G A 1981 *Phys. Rev. B* **23** 4369
- [33] van Elp J, Wieland J L, Eskes H, Kuiper P, Sawatzky G A, de Groot F M F and Turner T S 1991 *Phys. Rev. B* **44** 6090
- [34] Koitzsch A, Kraus R, Kroll T, Knupfer M, Büchner B, Batchelor D, Sun G L, Sun D L and Lin C T 2009 to be published
- [35] Sawatzky G A, Elfimov I S, van den Brink J and Zaanen J 2008 arXiv:0808.1390